

# Relativistic Quark Spin Coupling Effects in the Nucleon Electromagnetic Form Factors

W.R.B. de Araújo<sup>a</sup>, E.F. Suisso<sup>b</sup>, T. Frederico<sup>b</sup>, M. Beyer<sup>c</sup>, and H.J. Weber<sup>c\*</sup>

<sup>a</sup>*Laboratório do Acelerador Linear, Instituto de Física da USP*

*C.P. 663118, CEP 05315-970, São Paulo, Brazil*

<sup>b</sup>*Dep. de Física, Instituto Tecnológico de Aeronáutica, Centro Técnico Aeroespacial, 12.228-900 São José dos Campos, São Paulo, Brazil.*

<sup>c</sup>*FB Physik, Universität Rostock, 18051 Rostock, Germany*

## Abstract

We investigate the effect of different forms of relativistic spin coupling of constituent quarks in the nucleon electromagnetic form factors. The four-dimensional integrations in the two-loop Feynman diagram are reduced to the null-plane, such that the light-front wave function is introduced in the computation of the form factors. The neutron charge form factor is very sensitive to different choices of spin coupling schemes, once its magnetic moment is fitted to the experimental value. The scalar coupling between two quarks is preferred by the neutron data, when a reasonable fit of the proton magnetic momentum is found.

The purpose of this work is to study the nucleon electromagnetic form factors using different forms of relativistic spin coupling between the constituent quarks forming the nucleon. We use an effective Lagrangian to describe the quark spin coupling to the nucleon. We keep close contact with covariant field theory and perform a three-dimensional reduction of the amplitude for the photon absorption process by the nucleon to the null-plane,  $x^+ = x^0 + x^3 = 0$ , (see, e.g., Ref. [1]). After the three-dimensional reduction, one can introduce the nucleon light-front wave function in the two-loop momentum integrations which define the electromagnetic current. We consider the triangle diagram that is a major ingredient of recent electromagnetic and weak baryon form factor evaluations in light front dynamics.

We start with the effective Lagrangian for the N-q coupling

$$\mathcal{L}_{N-3q} = \alpha m_N \epsilon^{ijk} \bar{\Psi}_{(i)} i\tau_2 \gamma_5 \Psi_{(j)}^C \bar{\Psi}_{(k)} \Psi_N + (1 - \alpha) \epsilon^{ijk} \bar{\Psi}_{(i)} i\tau_2 \gamma_\mu \gamma_5 \Psi_{(j)}^C \bar{\Psi}_{(k)} i\partial^\mu \Psi_N + H.C. \quad (1)$$

where  $\tau_2$  is the isospin matrix, the color indices are  $\{i, j, k\}$  and  $\epsilon^{ijk}$  is the totally antisymmetric symbol. The conjugate quark field is  $\Psi^C = C\bar{\Psi}^\top$ , where  $C = i\gamma^2\gamma^0$  is the charge conjugation matrix;  $\alpha$  is a parameter to dial the spin coupling parameterization, and  $m_N$  is the nucleon mass.

---

\*permanent address: Dept. of Physics, University of Virginia, Charlottesville, U.S.A.

The macroscopic matrix element of the nucleon electromagnetic current  $j_N^+(Q^2)$  in the Breit-frame and in the light-front spinor basis is given by:

$$\begin{aligned} \langle s' | j_N^+(Q^2) | s \rangle &= \bar{u}(p', s') \left( F_{1N}(Q^2) \gamma^+ + i \frac{\sigma^{+\mu} Q_\mu}{2m_N} F_{2N}(Q^2) \right) u(p, s) \\ &= \frac{p^+}{m_N} \langle s' | F_{1N}(Q^2) + i \frac{F_{2N}(Q^2)}{2m_N} \vec{n} \cdot (\vec{q}_\perp \times \vec{\sigma}) | s \rangle, \end{aligned} \quad (2)$$

where  $F_{1N}$  and  $F_{2N}$  are the Dirac and Pauli form factors, respectively.  $\vec{n}$  is the unit vector along the z-direction. The Breit-frame momenta are  $Q^\mu = (0, \vec{q}_\perp)$ , such that ( $Q^+ = Q^0 + Q^3 = 0$ ) and  $\vec{q}_\perp = (q^1, q^2)$ ;  $p = (\sqrt{\frac{q_\perp^2}{4} + m_N^2}, -\frac{\vec{q}_\perp}{2})$  and  $p' = (\sqrt{\frac{q_\perp^2}{4} + m_N^2}, \frac{\vec{q}_\perp}{2})$ .

The light-front spinors are:

$$u(p, s) = \frac{\not{p} + m_N}{2\sqrt{p^+ m_N}} \gamma^+ \gamma^0 \begin{pmatrix} \chi_s^{\text{Pauli}} \\ 0 \end{pmatrix}. \quad (3)$$

The Dirac spinor of the instant form

$$u_D(p, s) = \frac{\not{p} + m_N}{\sqrt{2m(p^0 + m)}} \begin{pmatrix} \chi_s^{\text{Pauli}} \\ 0 \end{pmatrix} \quad (4)$$

carries the subscript  $D$ .

The Sachs form factors are defined by:

$$\begin{aligned} G_{EN}(Q^2) &= F_{1N}(Q^2) + \frac{Q^2}{4m_N^2} F_{2N}(Q^2), \\ G_{MN}(Q^2) &= F_{1N}(Q^2) + F_{2N}(Q^2). \end{aligned} \quad (5)$$

The magnetic moment is  $\mu_N = G_{MN}(0)$  and the mean square radius is  $r_N^2 = 6 \frac{dG_{EN}(Q^2)}{dQ^2} |_{Q^2=0}$ .

The nucleon electromagnetic current ( $j_N^+(Q^2)$ ), obtained from the effective Lagrangian by considering the complete antisymmetrization of the matrix element of the current, has five topologically distinct diagrams. We can calculate the photon absorption amplitude considering only the process on quark 3, due to the symmetrization of the microscopic matrix element after the factorization of the color degree of freedom. Figure (1a) defines the nucleon spin-space operator  $j_{aN}^+$  and represents the case where quark 3 absorbs the photon while 1 and 2 compose the spectator-coupled quark pair in Eq.(1) for the initial and final nucleons. In Figure (1b), the coupled quark pair in the initial nucleon is (13) and in the final nucleon the coupled pair is (12). The operator  $j_{bN}^+$ , represented by the diagram (1b), should be multiplied by a factor of 4. A factor 2 comes from the exchange of quarks 1 and 2, and another factor 2 comes from the invariance of this term under the exchange of the pairs in the initial and final nucleons, which is a consequence of time reversal invariance and parity transformation property. The operator  $j_{cN}^+$  is represented by figure (1c), where the initial coupled pair quark is (13) and the final coupled pair is (23). This operator is multiplied by a factor of 2 because the quarks 1 and 2 can be exchanged. The operator represented by diagram (1d),  $j_{dN}^+$ , corresponds to the process in which the photon is absorbed by the coupled quark pair (23) while 1 is spectator. In this case, two diagrams are possible by the

exchange of quarks 1 and 2. Thus, the microscopic operator of the nucleon current is given by the sum of four terms:

$$j_N^+(Q^2) = j_{aN}^+(Q^2) + 4j_{bN}^+(Q^2) + 2j_{cN}^+(Q^2) + 2j_{dN}^+(Q^2) . \quad (6)$$

The nucleon current operators  $j_{\beta N}^+$ ,  $\beta = a, b, c, d$ , are written directly from the Feynman diagrams of fig.1. The electromagnetic field is coupled in the usual minimal way ensuring gauge invariance. The electromagnetic current,  $j_N^+$ , is constructed from the Feynman triangle two-loop diagrams of figures (1a) to (1d):

$$\begin{aligned} \langle s' | j_{aN}^+(Q^2) | s \rangle &= -\langle N | \hat{Q}_q | N \rangle \text{Tr} [i\tau_2(-i)\tau_2] \int \frac{d^4 k_1 d^4 k_2}{(2\pi)^8} \Lambda(k_i, p') \Lambda(k_i, p) \bar{u}(p', s') S(k'_3) \gamma^+ \\ &\times S(k_3) u(p, s) \text{Tr} \left[ S(k_2) (\alpha m_N + (1 - \alpha) \not{p}) \gamma^5 S_c(k_1) \gamma^5 (\alpha m_N + (1 - \alpha) \not{p}') \right] , \quad (7) \end{aligned}$$

with  $S(p) = \frac{1}{\not{p} - m + i\epsilon}$ , and  $S_c(p) = \left[ \gamma^0 \gamma^2 \frac{1}{\not{p} - m + i\epsilon} \gamma^0 \gamma^2 \right]^\top$ .  $m$  is the constituent quark mass and  $k'_3 = k_3 + Q$ . The quark charge operator  $\hat{Q}_q$  is diagonal and its matrix elements are 2/3 for the up quark and -1/3 for the down quark. The choice of the function  $\Lambda(k_i, p)$  will be discussed later.

The diagram of figure (1b) is given by:

$$\begin{aligned} \langle s' | j_{bN}^+(Q^2) | s \rangle &= -\langle N | \hat{Q}_q | N \rangle \int \frac{d^4 k_1 d^4 k_2}{(2\pi)^8} \Lambda(k_i, p') \Lambda(k_i, p) \bar{u}(p', s') S(k'_3) \gamma^+ S(k_3) \\ &\times (\alpha m_N + (1 - \alpha) \not{p}) \gamma^5 S_c(k_1) \gamma^5 (\alpha m_N + (1 - \alpha) \not{p}') S(k_2) u(p, s) . \quad (8) \end{aligned}$$

The diagram of figure (1c) is given by:

$$\begin{aligned} \langle s' | j_{cN}^+(Q^2) | s \rangle &= \langle N | \hat{Q}_q | N \rangle \int \frac{d^4 k_1 d^4 k_2}{(2\pi)^8} \Lambda(k_i, p') \Lambda(k_i, p) \bar{u}(p', s') S(k_1) (\alpha m_N + (1 - \alpha) \not{p}) \\ &\times \gamma^5 S_c(k_3) \gamma^+ S_c(k'_3) \gamma^5 (\alpha m_N + (1 - \alpha) \not{p}') S(k_2) u(p, s) . \quad (9) \end{aligned}$$

The diagram of figure (1d) is given by:

$$\begin{aligned} \langle s' | j_{dN}^+(Q^2) | s \rangle &= -\text{Tr} [\hat{Q}_q] \int \frac{d^4 k_1 d^4 k_2}{(2\pi)^8} \Lambda(k_i, p') \Lambda(k_i, p) \bar{u}(p', s') S(k_2) u(p, s) \\ &\text{Tr} \left[ \gamma^5 (\alpha m_N + (1 - \alpha) \not{p}') S(k'_3) \gamma^+ S(k_3) (\alpha m_N + (1 - \alpha) \not{p}) \gamma^5 S_c(k_1) \right] . \quad (10) \end{aligned}$$

The light-front coordinates are defined as  $k^+ = k^0 + k^3$ ,  $k^- = k^0 - k^3$ ,  $k_\perp = (k^1, k^2)$ . In each term of the nucleon current, from  $j_{aN}^+$  to  $j_{dN}^+$ , the Cauchy integrations over  $k_1^-$  and  $k_2^-$  are performed. That means the on-mass-shell pole of the Feynman propagators for the spectator particles 1 and 2, in the photon absorption process, are taken into account. In the Breit-frame, with  $Q^+ = 0$ , there is a maximal suppression of light-front Z-diagrams in  $j^+$  [2,3]. Thus, the components of the momentum  $k_1^+$  and  $k_2^+$  are bounded, such that  $0 < k_1^+ < p^+$  and  $0 < k_2^+ < p^+ - k_1^+$  [4]. The four-dimensional integrations of Eqs.(7) to (10) are reduced to the three-dimensional volume of the null-plane.

The analytical integration of Eq.(7) of the '-' components of momentum yields:

$$\begin{aligned}
\langle s' | j_{aN}^+(Q^2) | s \rangle &= 2p^{+2} \langle N | \hat{Q}_q | N \rangle \int \frac{d^2 k_{1\perp} dk_1^+ d^2 k_{2\perp} dk_2^+}{4(2\pi)^6 k_1^+ k_2^+ k_3^+{}^2} \theta(p^+ - k_1^+) \theta(p^+ - k_1^+ - k_2^+) \\
&\quad \text{Tr} [(\not{k}_2 + m) (\alpha m_N + (1 - \alpha) \not{p}) (\not{k}_1 + m) (\alpha m_N + (1 - \alpha) \not{p}')] \\
&\quad \bar{u}(p', s') (\not{k}'_3 + m) \gamma^+ (\not{k}_3 + m) u(p, s) \frac{\Lambda(k_i, p')}{m_N^2 - M_0'^2} \frac{\Lambda(k_i, p)}{m_N^2 - M_0^2}, \quad (11)
\end{aligned}$$

where  $k_1^2 = m^2$  and  $k_2^2 = m^2$  and the free three-quark squared mass is defined by:

$$M_0^2 = p^+ \left( \frac{k_{1\perp}^2 + m^2}{k_1^+} + \frac{k_{2\perp}^2 + m^2}{k_2^+} + \frac{k_{3\perp}^2 + m^2}{k_3^+} \right) - p_\perp^2, \quad (12)$$

and  $M_0'^2 = M_0^2(k_3 \rightarrow k'_3, \vec{p}_\perp \rightarrow \vec{p}'_\perp)$ .

The other terms of the nucleon current, as given by Eqs. (8)-(10) are also integrated over the  $k^-$  momentum components of particles 1 and 2, following the same steps used to obtain Eq.(11) from Eq.(7):

$$\begin{aligned}
\langle s' | j_{bN}^+(Q^2) | s \rangle &= p^{+2} \langle N | \hat{Q}_q | N \rangle \int \frac{d^2 k_{1\perp} dk_1^+ d^2 k_{2\perp} dk_2^+}{4(2\pi)^6 k_1^+ k_2^+ k_3^+{}^2} \theta(p^+ - k_1^+) \theta(p^+ - k_1^+ - k_2^+) \\
&\quad \bar{u}(p', s') (\not{k}'_3 + m) \gamma^+ (\not{k}_3 + m) (\alpha m_N + (1 - \alpha) \not{p}) (\not{k}_1 + m) \\
&\quad \times (\alpha m_N + (1 - \alpha) \not{p}') (\not{k}_2 + m) u(p, s) \frac{\Lambda(k_i, p')}{m_N^2 - M_0'^2} \frac{\Lambda(k_i, p)}{m_N^2 - M_0^2}, \quad (13)
\end{aligned}$$

$$\begin{aligned}
\langle s' | j_{cN}^+(Q^2) | s \rangle &= p^{+2} \langle N | \hat{Q}_q | N \rangle \int \frac{d^2 k_{1\perp} dk_1^+ d^2 k_{2\perp} dk_2^+}{4(2\pi)^6 k_1^+ k_2^+ k_3^+{}^2} \theta(p^+ - k_1^+) \theta(p^+ - k_1^+ - k_2^+) \\
&\quad \bar{u}(p', s') (\not{k}_1 + m) (\alpha m_N + (1 - \alpha) \not{p}) (\not{k}_3 + m) \gamma^+ (\not{k}'_3 + m) \\
&\quad \times (\alpha m_N + (1 - \alpha) \not{p}') (\not{k}_2 + m) u(p, s) \frac{\Lambda(k_i, p')}{m_N^2 - M_0'^2} \frac{\Lambda(k_i, p)}{m_N^2 - M_0^2}, \quad (14)
\end{aligned}$$

$$\begin{aligned}
\langle s' | j_{dN}^+(Q^2) | s \rangle &= p^{+2} \text{Tr} [\hat{Q}_q] \int \frac{d^2 k_{1\perp} dk_1^+ d^2 k_{2\perp} dk_2^+}{4(2\pi)^6 k_1^+ k_2^+ k_3^+{}^2} \theta(p^+ - k_1^+) \theta(p^+ - k_1^+ - k_2^+) \\
&\quad \text{Tr} [(\alpha m_N + (1 - \alpha) \not{p}') (\not{k}'_3 + m) \gamma^+ (\not{k}_3 + m) (\alpha m_N + (1 - \alpha) \not{p}) (\not{k}_1 + m)] \\
&\quad \bar{u}(p', s') (\not{k}_2 + m) u(p, s) \frac{\Lambda(k_i, p')}{m_N^2 - M_0'^2} \frac{\Lambda(k_i, p)}{m_N^2 - M_0^2}. \quad (15)
\end{aligned}$$

The Gaussian wave function is introduced in Eqs.(11)-(15) through the substitution [2]:

$$\frac{1}{2(2\pi)^3} \frac{\Lambda(k_i, p)}{m_N^2 - M_0^2} \rightarrow N \exp(-M_0^2/2\beta^2), \quad (16)$$

where  $N$  is chosen such that the proton charge is 1.

The spin-flavor invariant of the nucleon with quark pair spin zero ( $\alpha = 1$ ) is the simplest of a basis of 8 such states given in greater detail in Ref. [5], for example. The only nucleon spin invariant used and tested in form factor calculations contains the additional projector  $\not{p} + M_0$  onto large Dirac components, a characteristic feature of the Bakamjian-Thomas

formalism [6]. The spin-flavor invariant in the effective Lagrangian, (1), with  $\alpha = 1/2$ , resembles the Bakamjian-Thomas, but is not equivalent to it, as it will be explained below.

As we have discussed, the residues of the triangle Feynman diagram are evaluated at the on- $k^-$ -shell poles of the spectator particles [4]. The numerator of the fermion propagator of the quark which absorbs the photon momentum can be considered on- $k^-$ -shell because  $(\gamma^+)^2 = 0$ . Thus, all the numerators of the fermion propagators can be substituted by the positive energy spinor projector, written in terms of light-front spinors. To explore the physical meaning of the effective Lagrangian, we follow closely the work of Ref. [7], where the case  $\alpha = 1$  is discussed in detail. It has been suggested to perform a kinematical light-front boost of the matrix elements of the spin operators between quark states and quark-nucleon states, related to the initial and final nucleons and their respective rest-frames. Because the Wigner rotation is unity for such Lorentz transformations, the matrix elements appearing in the nucleon electromagnetic current, corresponding to the spin coupling of the quarks to the initial or final nucleon, can be evaluated in their respective rest-frames. A typical matrix element of the spin coupling coefficient for  $\alpha = 1$  appearing in the evaluation of  $j^+$ , when calculated in the nucleon rest frame, is given by:

$$\chi(s_1, s_2, s_3; s_N) = \bar{u}_1 \gamma_5 u_2^C \bar{u}_3 u_N, \quad (17)$$

where  $u_i = u(k_i, s_i)$  is the light-front spinor for the  $i$ -th quark.

To calculate Eq. (17), we begin by evaluating the matrix element of the pair coupled to spin zero in the rest frame of the pair (c.m.) which, again, is found by a kinematical light-front boost from the nucleon rest frame. Because the Wigner rotation is unity for such a Lorentz transformation, we can write (viz.  $u_{c.m.}(\vec{k}^{c.m.}, s) = u(\vec{k}^{c.m.}, s)$ ):

$$\begin{aligned} I(s_1, s_2, 0) &= \bar{u}(\vec{k}_1, s_1) \gamma_5 u^C(\vec{k}_2, s_2) \\ &= \bar{u}(\vec{k}_1^{c.m.}, s_1) \gamma_5 u^C(\vec{k}_2^{c.m.}, s_2), \end{aligned} \quad (18)$$

where  $\vec{k}^{c.m.} = (k^{+c.m.}, \vec{k}_\perp^{c.m.})$  are the kinematical momentum variables of each particle 1 or 2 in the rest frame of the pair 12,  $k^{(c.m.)\mu} = (\Lambda k)^\mu$ . The particle momenta in the pair rest frame are obtained by a kinematical light-front transformation from those in the nucleon rest frame to the pair rest frame. Introducing the completeness relation for positive energy Dirac spinors in Eq. (18), one finds:

$$\begin{aligned} I(s_1, s_2, 0) &= \sum_{\bar{s}_1 \bar{s}_2} \bar{u}(\vec{k}_1^{c.m.}, s_1) u_D(\vec{k}_1^{c.m.}, \bar{s}_1) \bar{u}_D(\vec{k}_1^{c.m.}, \bar{s}_1) \\ &\quad \gamma_5 C \bar{u}_D^\top(\vec{k}_2^{c.m.}, \bar{s}_2) \left( \bar{u}(\vec{k}_2^{c.m.}, s_2) u_D(\vec{k}_2^{c.m.}, \bar{s}_2) \right)^\top. \end{aligned} \quad (19)$$

The Clebsch-Gordan coefficients are found by using the Dirac spinors in Eq.(19)

$$\bar{u}_D(\vec{k}_1^{c.m.}, \bar{s}_1) \gamma_5 C \bar{u}_D^\top(\vec{k}_2^{c.m.}, \bar{s}_2) \rightarrow \chi_{\bar{s}_1}^\dagger i \sigma_2 \chi_{\bar{s}_2}^* = \sqrt{2} \langle \frac{1}{2} \bar{s}_1 \frac{1}{2} \bar{s}_2 | 00 \rangle. \quad (20)$$

The Melosh rotation is given by:

$$[R_M(p)]_{s't} = \bar{u}_D(p, s') u(p, s). \quad (21)$$

From Eqs.(17), (19), (20), and (21), the form of the spin coupling of the nucleon to the quarks is written as:

$$\chi(s_1, s_2, s_3; s_N) = \sum_{\bar{s}_1 \bar{s}_2} \left[ R_M^\dagger(\vec{k}_1^{c.m.}) \right]_{s_1 \bar{s}_1} \left[ R_M^\dagger(\vec{k}_2^{c.m.}) \right]_{s_2 \bar{s}_2} \left[ R_M^\dagger(\vec{k}_3) \right]_{s_3 s_N} \chi_{\bar{s}_1}^\dagger i\sigma_2 \chi_{\bar{s}_2}^*. \quad (22)$$

The Melosh rotations of the spin-zero coupled pair (12) have the momentum arguments evaluated in the rest frame of the pair in Eq. (22), while in the BT construction the arguments of the Melosh rotations are all evaluated in the nucleon rest frame. Moreover, the light-front spinors in Eqs.(18),(19) are no longer all in the nucleon rest frame, which will have observable consequences in the electromagnetic form factors. Also, the various total momentum '+' components, such as  $p_{12}^+$  and  $p^+$  now appear in different frames, whereas in the BT case only  $M_0$  occurs for  $p^+$  in the nucleon rest frame.

The same considerations will apply to the pair-spin 0 invariant with an additional  $\not{p} + m_N$  ( $\alpha = 1/2$ ) from the projector which reduces to  $\gamma_0 + 1$  in the nucleon rest frame. However, the Melosh rotations have as arguments the quark momenta in the nucleon rest-frame. This last case still differs from the BT construction because the sum of the '+' components of the quark momenta is the nucleon momentum,  $p^+$ , and not  $M_0$  as in the BT formalism. After this formal discussion, in next we discuss the observable effects of different choices of quark spin coupling schemes for the nucleon electromagnetic current.

The numerical results for the nucleon electromagnetic form-factors for  $\alpha = 1, 0$  and  $1/2$  are discussed in the following. The quark mass is 220 MeV [8]. In our calculations the size parameter  $\beta$  is adjusted such that the neutron magnetic moment becomes  $-1.91 \mu_N$ . This choice of parameterization through the neutron magnetic moment was used in order to focus our study on the electric neutron form factor, which turns out to be very sensitive to different spin coupling schemes. In Table I, the results are shown for the nucleon mean square radius and proton magnetic moment. The neutron mean square radius depends strongly on the spin coupling parameter  $\alpha$ . The best result for the neutron mean square radius is found for  $\alpha = 1$ , i.e., the scalar coupling of the quark pair. The proton observables are just consistent with the data. However, a simultaneous fit of the nucleon magnetic moments and mean square radii does not seem possible with good precision.

In figure 2, we present the model results for the neutron electric form-factor  $G_{En}$ , and the scalar coupling is shown to be consistent with data. The calculation with  $\alpha = 1/2$  is below the data as anticipated from the small radius. The calculation with  $\alpha = 0$  yields a negative  $G_{En}$  and it was not shown in the figure. The model results for  $G_{Mn}$  is compared to the data in figure 3. Below momentum transfers of 1 GeV/c, the model is consistent with the experimental data and above this value it deviates from the data. The difference between the model and experimental values of  $G_{Mn}$  could be minimized, at the expense of increasing the deviation of the neutron mean square radius from its experimental value.

In figure 4, we show the ratio of the proton electric to magnetic form factors compared with recent data. The choice of  $\alpha = 1$ , among the values of 1,  $1/2$  and 0, shows the smallest deviation from the data. However, the calculation still misses the experimental values which could be finally fitted introducing constituent quarks form factors [8], but this is beyond our purpose in this work.

In conclusion, we have tested different spin coupling schemes for the nucleon in a calculation of the nucleon electromagnetic form factors. We find that the electric form factor

of the neutron can be used to constrain the quark spin coupling schemes. The comparison with the neutron data below momentum transfer of 1 GeV/c suggests that the scalar pair is preferred in the relativistic quark spin coupling of the nucleon.

**Acknowledgments:** HJW is grateful to G. Röpke and the many particle research group for their warm hospitality. WRBA thanks CNPq for financial support and LCCA/USP for providing computational facilities, EFS thanks FAPESP for financial support and TF thanks CNPq, FAPESP and CAPES/DAAD/PROBRAL.

## REFERENCES

- [1] J. Carbonell, B. Desplanques, V. Karmanov and J.-F. Mathiot, Phys. Reports **300** (1998) 215 , and references therein.
- [2] T. Frederico and G.A. Miller, Phys. Rev. **D45** (1992) 4207.
- [3] J.P.B.C de Melo, H.W. Naus and T. Frederico, Phys. Rev. **C59** (1999) 2278.
- [4] J.P.B.C. de Melo and T. Frederico, Phys. Rev. **C55** (1997) 2043, and references therein.
- [5] M. Beyer, C. Kuhrts, and H. J. Weber, Ann. Phys. (NY) **269** (1998) 129, and references therein.
- [6] B. Bakamjian and L. H. Thomas, Phys. Rev. **92** (1953) 1300.
- [7] W.R.B. de Araújo, M. Beyer, T. Frederico and H.J. Weber, J. Phys. **G 25** (1999) 158.
- [8] F. Cardarelli, E. Pace, G. Salme and S. Simula, Phys. Lett. **B357** (1995) 267; Few Body Syst. Suppl. 8 (1995) 345; F. Cardarelli and S. Simula, nucl-th/9906095.
- [9] S. Kopecky et al., Phys. Rev. Lett. **74** (1995) 2427.
- [10] S.J. Brodsky and J.R. Primack, Ann. Phys. (N.Y.) **52** (1969) 315.
- [11] J.J. Murphy II, Y.M. Shin, and D.M. Skopik, Phys. Rev. **C9** (1974) 3125.
- [12] S.Platchkov et al., Nucl.Phys. A510 (1990) 740.
- [13] W. Albrecht et al., Phys. Lett. B26 (1968) 642.
- [14] S. Rock et al., Phys. Rev. Lett. 49 (1982) 1139.
- [15] A.Lung et al., Phys. Rev. Lett. 70 (1993) 6.
- [16] E.E.W. Bruins et al., Phys. Rev. Lett. (1995) 1.
- [17] S. Rock et al., Phys. Rev. Lett. **49** (1982) 1139.
- [18] T. Eden et al., Phys. Rev. **C50** (1994) R1749; M. Meyerhoff et al., Phys. Lett. **B327** (1994) 201; C. Herberg et al., Eur. Phys. J. **A5** (1999) 131; I. Passchier et al., Phys. Rev. Lett. **82** (1999) 4988; M. Ostrick et al., Phys. Rev. Lett. **83** (1999) 276; G. Becker et al. submitted to Eur. Phys. J.
- [19] C. Perdrisat, (TJLAB E93-27); priv. comm..



TABLES

TABLE I. Nucleon low-energy electromagnetic observables for different spin coupling parameters with a gaussian light-front wave function adjusted to  $\mu_n = -1.91\mu_N$ .

| $\alpha$ | $\beta(\text{MeV})$ | $\langle r^2 \rangle_n (\text{fm}^2)$ | $\langle r^2 \rangle_p (\text{fm}^2)$       | $\mu_p(\mu_N)$ |
|----------|---------------------|---------------------------------------|---|----------------|
| 1        | 562                 | -0.075                                | 0.877                                       | 3.11           |
| 1/2      | 664                 | -0.024                                | 0.718                                       | 3.05           |
| 0        | 661                 | 0.079                                 | 0.686                                       | 2.90           |
| Exp.     | -                   | $-0.113 \pm 0.005$ [9]                | $0.66 \pm 0.06$ [10] , $0.74 \pm 0.02$ [11] | 2.79           |

FIGURES

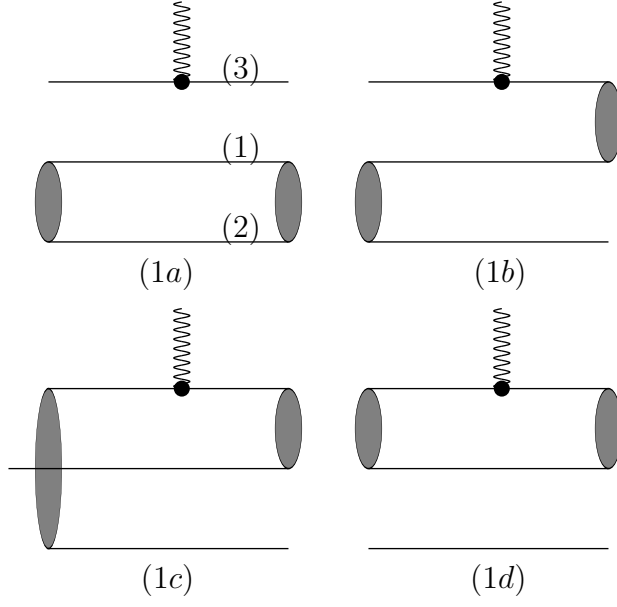
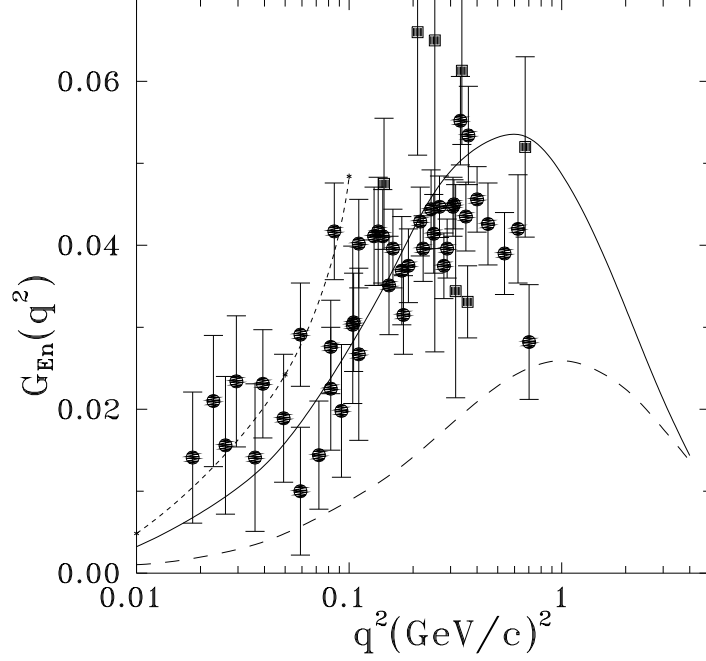
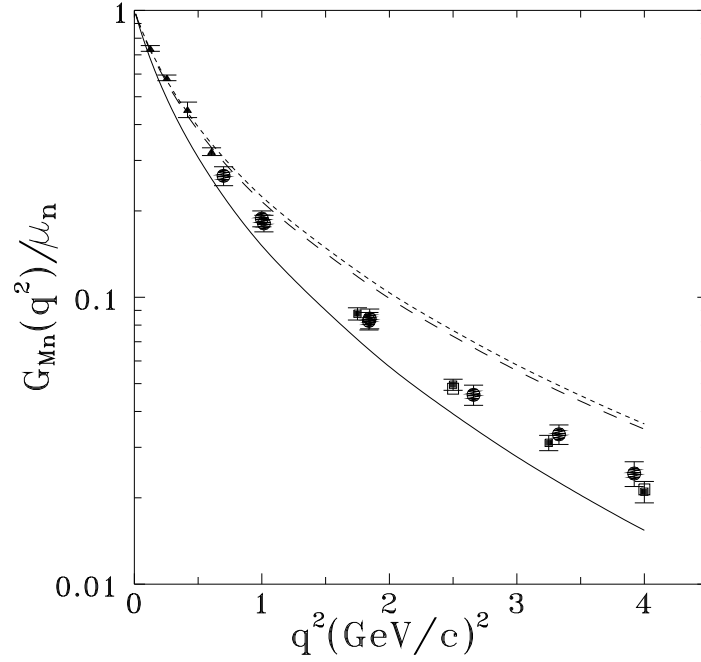


FIG. 1. Feynman diagrams for the nucleon current. The gray blob represents the spin invariant for the coupled quark pair in the effective Lagrangian, Eq. (1). Diagram (1a) represents  $j_{aN}^+$ , Eq.(7). Diagram (1b) represents  $j_{bN}^+$ , Eq.(8). Diagram (1c) represents  $j_{cN}^+$ , Eq.(9). Diagram (1d) represents  $j_{dN}^+$ , Eq.(10).



**Fig. 2** Neutron electric form factor as a function of the momentum transfer  $q^2 = -Q^2$ . Results for  $\alpha = 1$ , solid line; for  $\alpha = 1/2$ , dashed line. The short-dashed line represents the curve  $G_{En}(Q^2) \approx \frac{1}{6} \langle r^2 \rangle_n Q^2$  with the experimental value of  $\langle r^2 \rangle_n = -0.113 \text{ fm}^2$  [9]. The full circles are the experimental data from Ref. [12] and the full squares from Ref. [18].



**Fig. 3** Neutron magnetic form-factor as a function of the momentum transfer  $q^2 = -Q^2$ . Model results for  $\alpha = 1$ , solid line; for  $\alpha = 1/2$ , dashed line; for  $\alpha = 0$ , short-dashed line. Experimental data from Ref. [13], full circles; from Ref. [17], empty squares; from Ref. [15], full squares; from Ref. [16], full triangles.

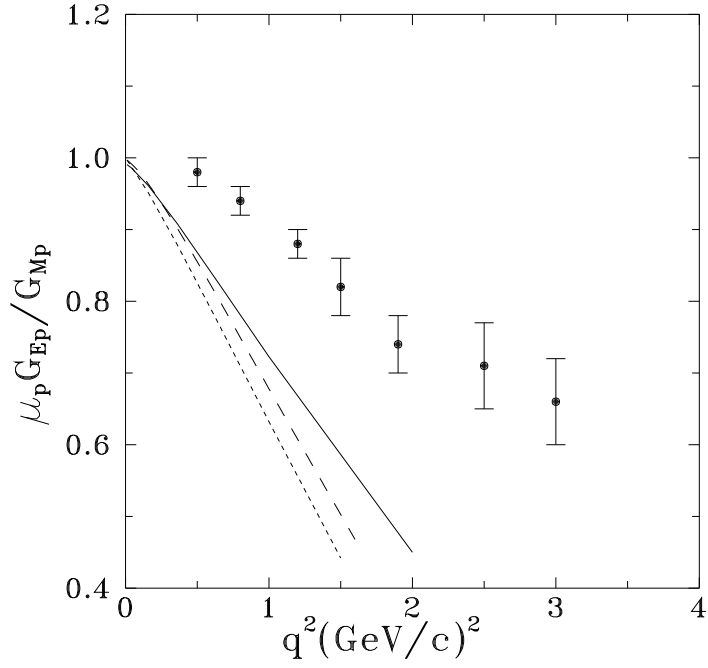


**Fig. 4** Proton form-factor ratio  $\mu_p G_{Ep}/G_{Mp}$  as a function of momentum transfer. Theoretical curves labeled as in figure 3. The experimental data comes from Ref. [19].